

Supplemental Information for:

Low energy expenditure at the edge of a seabird's winter range suggests energy underpins the Abundant Centre Hypothesis

Table of Contents:

Section 1: Study population and logger deployment	Page 2
Section 2: Geolocation light data processing	Page 3
Figure S1: Sun elevation angle selection (graphs)	Page 7
Figure S2: Sun elevation angle selection (tracks)	Page 8
Figure S3: Location distribution from geolocators vs IRMS algorithm	Page 9
Figure S4: Movement rate against time elapsed between locations	Page 9
Figure S5: Distribution of conductivity counts during nighttime	Page 10
Figure S6: Daily Budget activity during daytime, nighttime and twilight	Page 11
Table S1: Beta regression models for each behavioural response	Page 12
Figure S7: Predictions from beta regression models	Page 13
Figure S8: Heatmap of wind intensity	Page 14
Figure S9: Heatmap of sea surface temperature	Page 14

Section 1: Study population and logger deployment

The studied population is a long-term monitored colony located in Kongsfjorden, Svalbard (High Arctic Norway; 78° 54' N, 12° 12' E). During the study period (2008 to 2019), nest content monitoring was conducted at the colony every two to six days. We used the success of rearing at least one chick for 10 days after hatching (hereafter 'reproductive success') as a proxy of individual fitness. Three quarters of kittiwake chick mortality occurs within 10 days after hatching (Coulson & Porter, 1985) and, in some years, monitoring of nests had to stop before chicks fledged, so we considered this measurement to be representative of reproductive success. The sex of individuals was determined by molecular sexing following Fridolfsson and Ellegren (1999) or when paired with a known-sex partner.

We used geolocators (Global Location Sensors, GLS) to track the non-breeding movements of kittiwakes. From 2008 to 2019, adults were captured on their nests using a noose attached to a fishing rod and equipped with geolocators. We used mk18 and mk13 (British Antarctic Survey), mk4083 and mk4093 (Biotrack) and Intigeo F100 and C65 (Migrate Technology) mounted on a Darvic leg band. Devices measured light intensity every minute and recorded the maximum light intensity every 5 or 10 min. They also measured saltwater immersion (that we used as a proxy for bird activity, i.e., whether or not the bird was in contact with the sea water) every 3 or 30 s and stored the number of wet measurements within every 10 min period.

We recaptured 83% of the individuals at their return to the colony and recovered the geolocators. The estimated adult survival rate at the study site is 85%, suggesting that the geocator recovery rate closely reflected the expected adult return rate (Goutte et al., 2015). Only complete annual tracks were used in the analyses after filtering out tracks without saltwater immersion data and partial tracks caused by device failure or battery discharge. Two tracks were discarded because the kittiwake likely spent time on land as indicated by extensive periods of low saltwater immersion associated with stationary positions along the coast. This

pattern was not observed in any other tracks. Overall, we acquired 176 complete tracks from 117 different individuals (see Fig. 1, 55 females and 62 males), covering 11 non-breeding seasons, continuously (fall 2008 to spring 2019).

Our study does not include data on mortality because the tracking devices we used require the recapture of individuals to recover the data, meaning that particularly poor strategies (e.g., energetically costly strategies) may have been excluded from the dataset via early-life mortality. Particularly, juveniles may use an exploration and route refinement approach to migration (Guilford et al., 2011), so that breeding adults' strategy may be good enough not to impact breeding success. However, adult mortality mostly occurs in winter and the link between energy expenditure and survival is clear and well studied (Grosbois & Thompson, 2005; Mysterud et al., 2001; Woodworth et al., 2017). We could thus expect that a potential spatial trend in mortality across the winter range would parallel trends in individual energy expenditure and reproductive success.

Section 2: Geolocation light data processing – detailed methods from Léandri-Breton et al. (2021)

To infer geographic positions, geolocator data were processed according to the procedure developed for the SEATRACK project (Bråthen et al., 2021) and based on the threshold method calculating positions from twilight events ('coord' function from *GeoLight* package; Hill & Braun, 2001; Lisovski et al., 2020; Lisovski & Hahn, 2012). The procedure automatically identifies twilight events from raw light data ('twilightCalc' function from *GeoLight* package; Lisovski & Hahn, 2012) and applies a set of filters to twilight events (removing or moving events from false day/night detections or noise) and positions (speed, distribution limits, angle filter). Thus, all the geolocator data were processed automatically and consistently for all years of the study. Because light sensors from different geolocator models may differ, each track was calibrated individually. As such, the calibration method avoided systematic bias in latitude related to

potential differences in light sensors among geolocator models or years of production. Based on the approach by Hanssen et al., (2016) and van Bemmelen et al., (2019), the calibration method used a set of criteria that allowed calibration of tracks from kittiwakes breeding in the Arctic (79° N), where constant daylight prevents calibration at the time of deployment and recapture. By plotting the latitude against time for a range of sun elevation angles and for each track (Fig. S1), the sun elevation angle that was manually selected (1) minimized the amplification of the latitudinal error close to the equinoxes, (2) resulted in matching latitudes at both sides of the equinox, (3) resulted in positions that fitted the latitude of the colony at the beginning and the end of the track and (4) fitted the shape and position of the oceans and continents when plotting the positions on a map (Fig. S2). The method also included rooftop calibration of geolocator models, with the purpose to select model specific thresholds that would result in approximately the same sun elevation angles among geolocator models. The mk-series geolocators from the British Antarctic Survey and Biotrack were assigned a threshold of 1 unit, while Intigeo geolocators from Migrate Technology were assigned a threshold of 11 units.

Although longitudes can still be determined reliably around the equinoxes, estimation of latitudes is inherently imprecise during this period, because day length is similar around the globe (Lisovski et al., 2012). Therefore, locations around equinoxes were excluded (8 Sep–20 Oct, 20 Feb–3 Apr; Bråthen et al., 2021). Additionally, continuous daylight during the polar summer (or continuous night during polar winter) does not allow geolocation-based tracking using light-level sensors. To fill these gaps and reduce biases along the trajectories, missing locations were re-estimated by interpolation between known locations using an algorithm that was specifically developed for SEATRACK (Fauchald et al., 2019, see Fig. S3), based on a method originally proposed by Technitis et al., (2015). In short, this algorithm is based on the determination of so-called space-time prisms, which are 3-dimensional volumes defined by the coordinates (x,y) and time (z). The space-time prism delineates all the potential paths that can

be followed by an individual moving from point A to point B, given 3 parameters: the distance from A to B, the time budget available, and the maximum rate of movement (Miller, 1991). When projected onto a 2-dimensional plane, the space-time prism becomes the potential point area (hereafter *Ppa*; Technitis et al., 2015). Although the 3-dimensional representation of the space-time prism is useful to understand its concept (Neutens et al., 2007), it is naturally more convenient to work with only 2 dimensions when dealing with discrete time steps, as is the case in tracking studies, where locations are obtained at specific time intervals. Computing the *Ppa* in this context is straightforward (Technitis et al., 2015), given that the 3 above-mentioned parameters are known. Let us consider a startpoint (A) and start time (t_{i-1}), and an endpoint (B) and end time (t_{i+1}). Knowing the maximum rate of movement and the time t_i at which a new location (N_i) is to be created, one can determine the circle defining the maximum range (rg_{i-1}) from point A to the new location and the circle defining the maximum range (rg_{i+1}) to point B, centered on B. The *Ppa* corresponds to the area of overlap between those 2 circles of maximum range, i.e. the area delimiting all locations that are reachable from both A and B, given the time budget and maximum movement rate. This process can be repeated any number of times, depending on the number of new locations that need to be generated. The new locations are generated in a random order (i.e. not chronological), thus creating a sort of correlated random walk respecting the constraints set by the relative position of A and B, the time budget, and the maximum movement rate. Here, we used a dynamic value for the maximum movement rate parameter, based on the distribution of observed movement rates as a function of time elapsed between 2 locations from the dataset. To do so we calculated, based on each individual track, the movement rates for random combinations of known locations separated by varying time-intervals. We used the 75th percentile from that distribution as the maximum movement rate (Fig. S4). The 75th percentile was computed by quantile regression, using the function 'rq' from package *quantreg* (Koenker, 2020). Finally, the algorithm uses additional information to constrain the new positions obtained: (1) immersion data to

determine attendance at the colony and force a new location to remain close to the colony during the breeding season, (2) land masks (land filters) to constrain positions over the ocean, (3) longitudes (obtained from the geolocator data, as longitude can still be estimated during the equinoxes), and (4) light levels to determine whether the new position was north of the latitudinal limit of the polar day in summer or night in winter (i.e. continuous day/night recorded by the loggers).

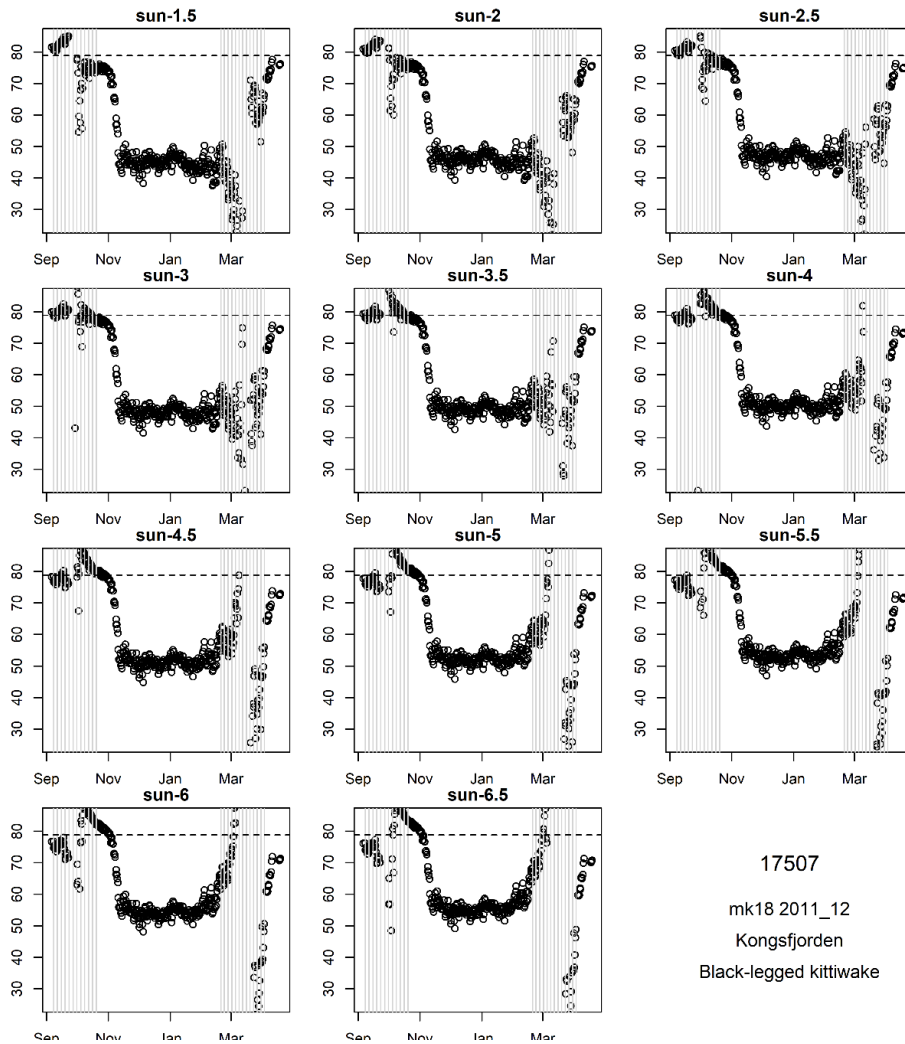


Figure S1: Example of sun elevation angle selection from Bråthen et al. (2021) for a black-legged kittiwake track (June 2011 to June 2012). For each annual track, latitude versus time is plotted for different sun elevation angles and the sun elevation angle selected 1) minimized the amplification of the latitudinal error close to the equinoxes, 2) resulted in matching latitudes at both sides of the equinox and 3) resulted in positions that fitted the latitude of the colony (Kongsfjorden, Svalbard; 78°5'N) at the beginning and the end of the track. In this example, we selected -3.0° as the appropriate sun elevation angle mainly from criteria 1) and 3) since the bird moved north during the spring equinox period, making criteria 2) less useful here. The horizontal dotted line shows the latitude of the colony, and the vertical grey lines indicate the periods around autumn and spring equinoxes.

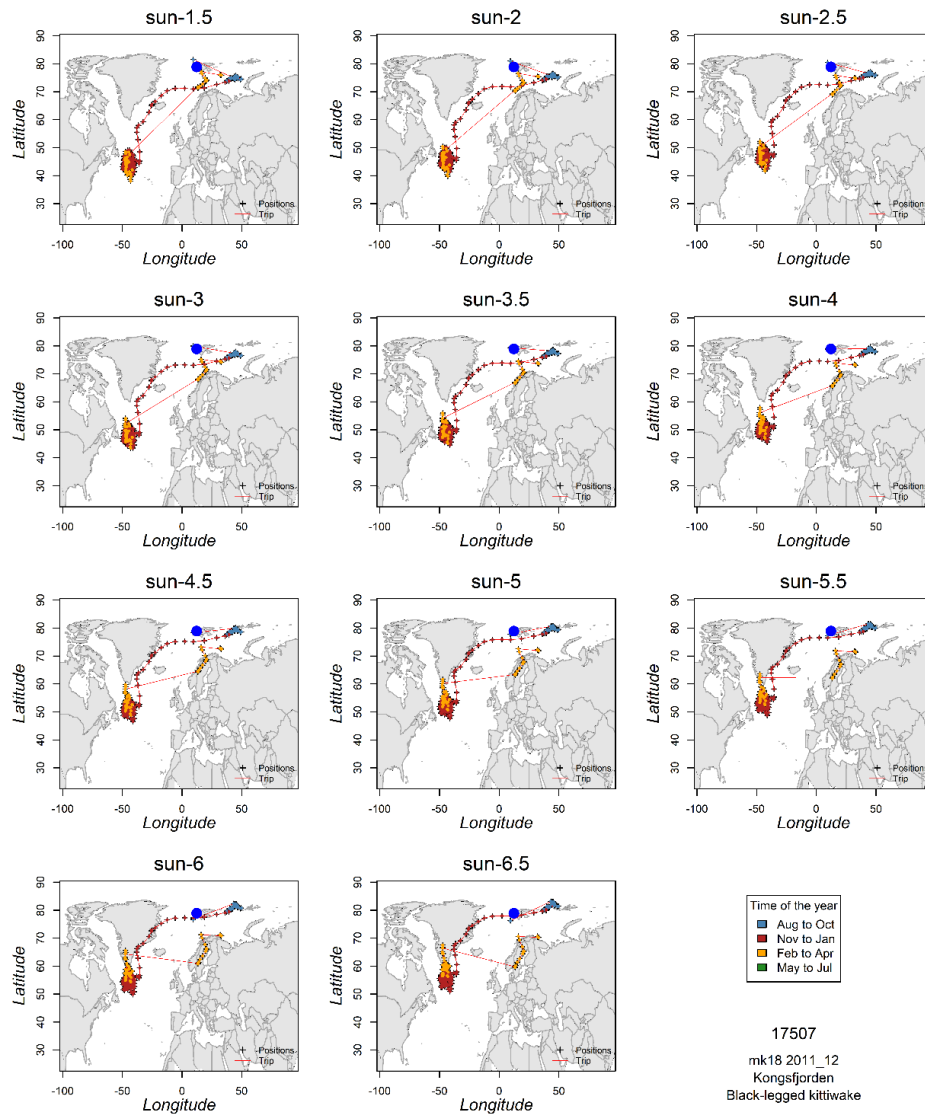


Figure S2: Example of sun elevation angle selection from Bråthen et al. (2021) for a black-legged kittiwake track (same track as in Figure S1). Smoothed and filtered positions calculated with different sun elevation angles. In combination with the steps illustrated in Figure S1, these maps supported the selection of -3.0° as sun elevation angle as it resulted in a track that best fitted the shape and position of the oceans and continents. The location of the colony (Kongsfjorden, Svalbard; 78°N , 12°E) is marked with a filled blue symbol, and positions are coloured by month. Positions from the equinox periods have been excluded from the map.

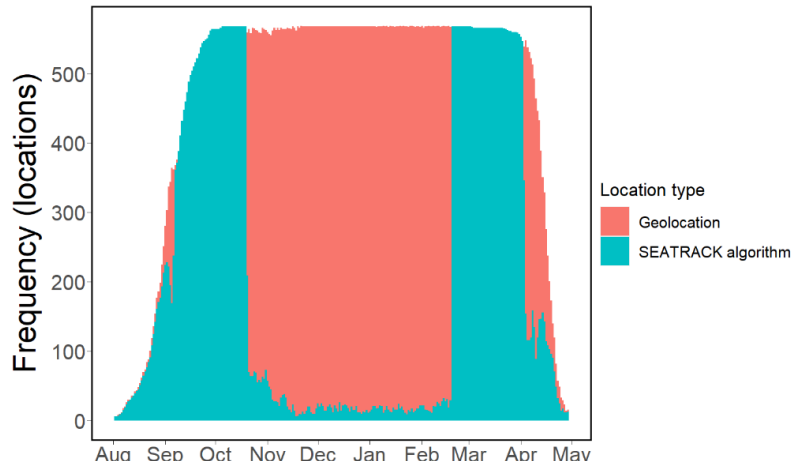


Figure S3: Frequency distribution of daily locations of black-legged kittiwakes estimated from the geolocation data only and those re-estimated with the algorithm IRMA developed for the SEATRACK program, over the tracking period.

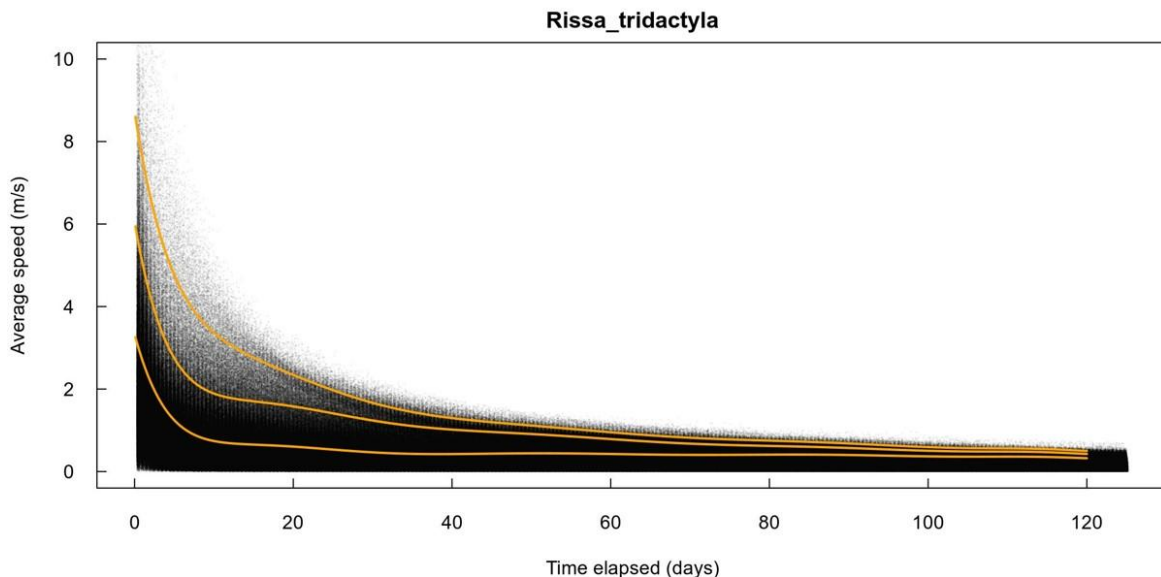


Figure S4: Movement rate plotted against time elapsed between two locations, for black-legged kittiwakes. The orange curves represent the 99th, 95th, and 75th percentiles predicted from a quantile regression model. The more conservative 75th percentile (lower regression curve) was selected for further analyses.

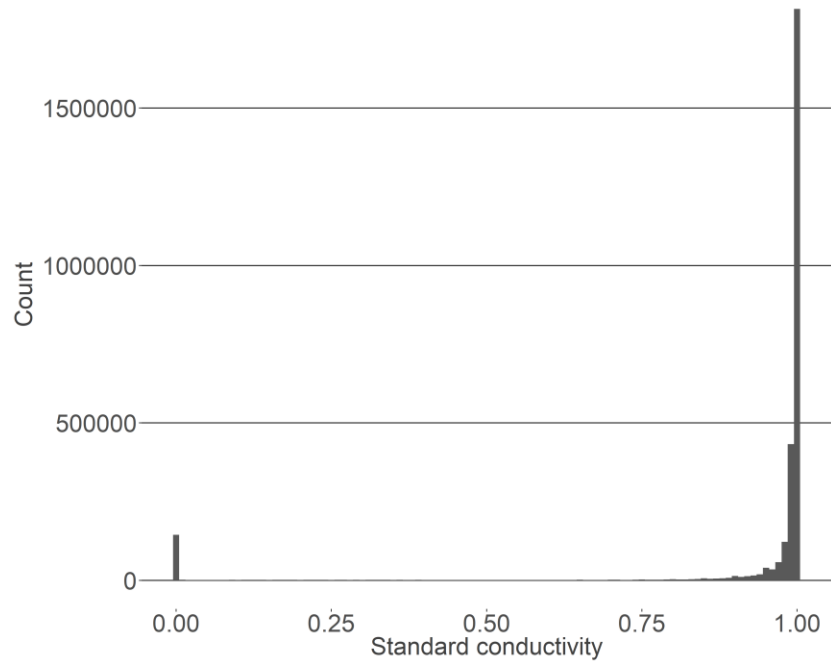


Figure S5: Distribution of standard conductivity counts during nighttime showing very high standard saltwater immersions associated to resting behaviour on water. To take this into account and avoid a bias towards foraging at night, a threshold of $0 < \text{standard conductivity} < 0.98$ was defined to identify the foraging activity periods. Nighttime periods were estimated after excluding the nautical twilights (6° and 12° below the horizon).

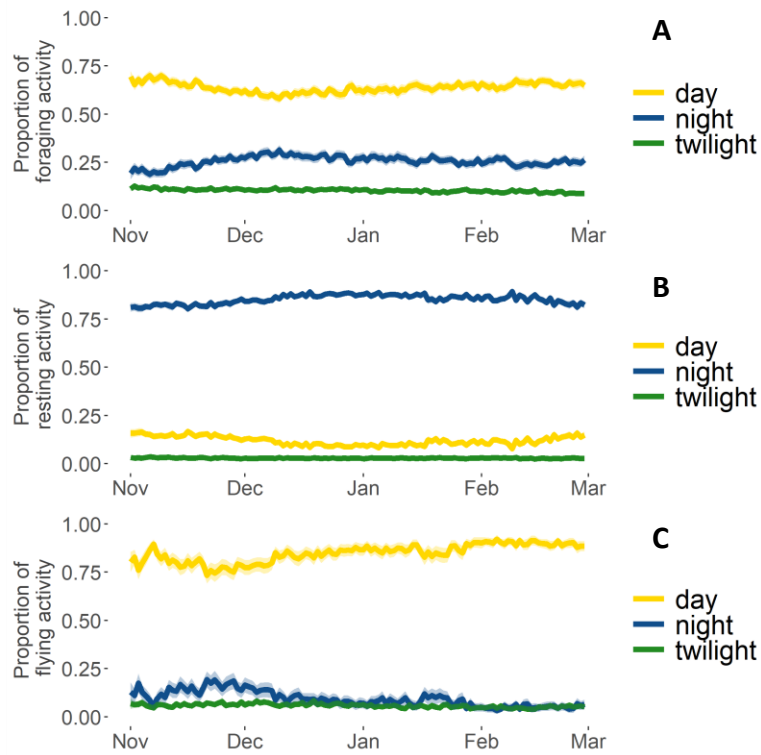


Figure S6: Proportion of time spent daily (A) foraging, (B) resting and (C) flying during the daytime, night time and twilight time over the non-breeding period. These periods were determined based on the nautical twilights (6° and 12° below the horizon).

Table S1: Results from beta regression models for each behavioural response, i.e. the proportions of time flying, foraging and resting in averaged over a 24-hr period. The coefficients of the predictors are reported, along with the standard error, the *p*-value and the 95% confidence intervals. Statistically significant interactions are reported in bold. In all three models, the individual identification and the year were included as random factors.

Response	Predictors	Coef	SE	<i>p</i> -value	95% CI
Flying time (daily proportion)	Distance to range centre (km)	-0.0001	0.00001	<0.0001	[-0.00010, -0.00007]
	Mean daylength (scaled)	-0.03	0.02	0.02	[0.004, 0.05]
	Sex (male vs female)	-0.004	0.026	0.9	[-0.06, 0.05]
Foraging time (daily proportion)	Distance to range centre (km)	0.00008	0.00001	<0.0001	[0.00004, 0.00011]
	Mean daylength (scaled)	0.04	0.01	<0.001	[0.16, 0.06]
	Sex (male vs female)	-0.06	0.03	0.02	[-0.11, -0.01]
Resting time (daily proportion)	Distance to range centre (km)	0.000001	0.00001	1.0	[-0.00003, 0.00003]
	Mean daylength (scaled)	-0.05	0.01	<0.0001	[-0.07, -0.03]
	Sex (male vs female)	0.05	0.02	0.003	[0.005, 0.10]

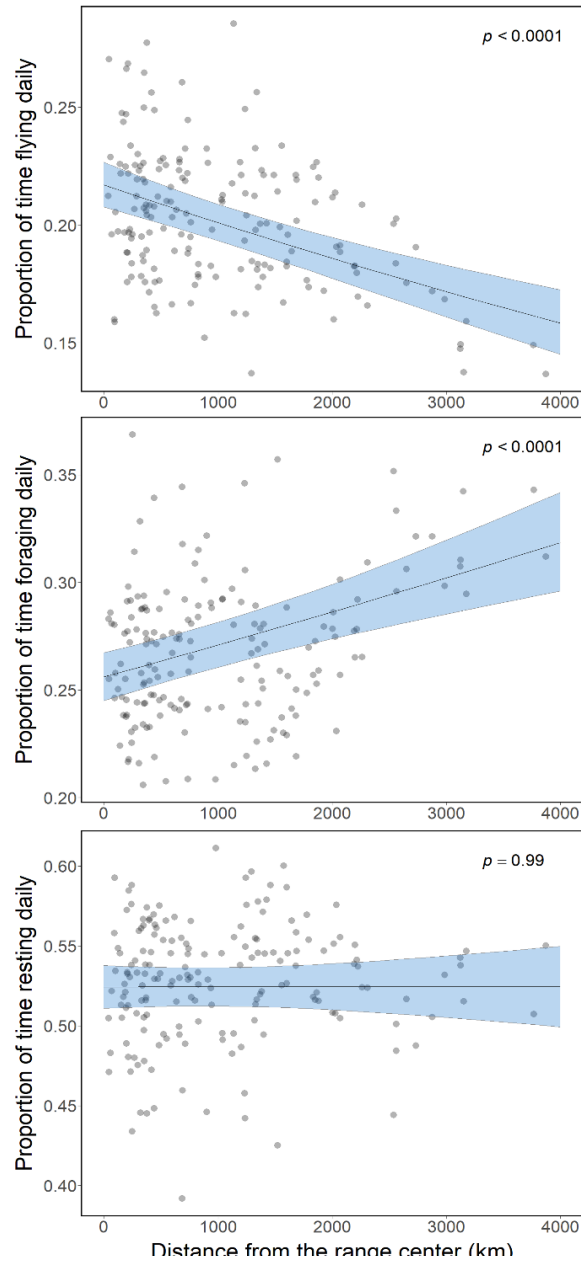


Figure S7: Proportion of time spent A) flying, B) foraging and C) resting over a 24-hr period over the distance from the centre of the population’s wintering range. Plots show the predictions from beta regression models with their 95% confidence intervals, over the jittered raw data. In all three models, the individual identification and the year were included as random factors.

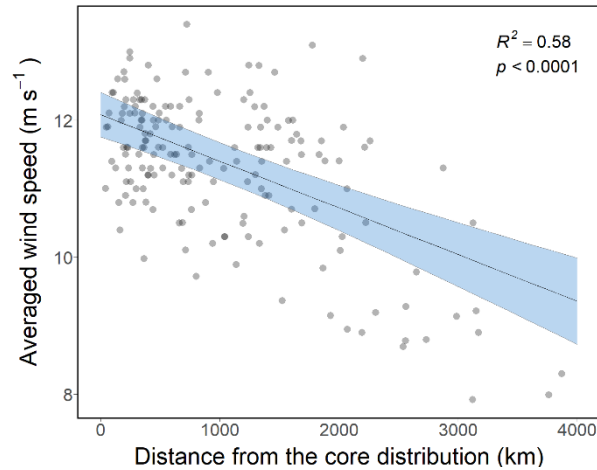


Figure S8: Wind intensity (m s^{-1}) experienced by individuals during winter as a function of distance from the center of the population's winter distribution. The plot shows predictions from an LMM, with latitudes and longitudes of individuals' wintering centroids included as fixed effects. Individual identity and year of tracking are included as random effects.

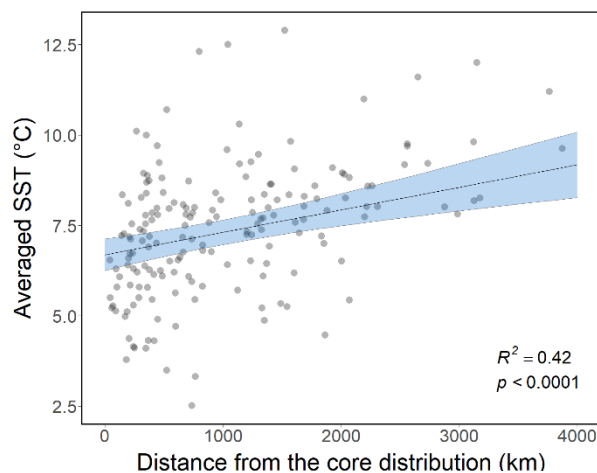


Figure S9: Sea surface temperature (SST) experienced by individuals during winter as a function of distance from the center of the population's winter distribution. The plot shows predictions from an LMM, with latitudes and longitudes of individuals' wintering centroids included as fixed effects. Individual identity and year of tracking are included as random effects.

REFERENCES

- Bråthen, V. S., Moe, B., Amélineau, F., Ekker, M., Fauchald, P., Helgason, H. H., Johansen, M. K., Merkel, B., Tarroux, A., & Åström, J., Strøm, H. (2021). *An automated procedure (v2.0) to obtain positions from light-level geolocators in large-scale tracking of seabirds. A method description for the SEATRACK project. NINA Report 1893. Norwegian Institute for Nature Research.* <https://hdl.handle.net/11250/2735757>
- Coulson, J. C., & Porter, J. M. (1985). Reproductive success of the Kittiwake. *Ibis*, *127*, 450–466.
- Fauchald, P., Tarroux, A., Bråthen, V. S., Descamps, S., Ekker, M., Helgason, H. H., Merkel, B., Moe, B., Åström, J., & Strøm, H. (2019). *Arctic-breeding seabirds' hotspots in space and time - A methodological framework for year-round modelling of environmental niche and abundance using light-logger data. NINA Report 1657. Norwegian Institute for Nature Research (NINA) (Issue April).* <http://hdl.handle.net/11250/2595504>
- Fridolfsson, A.-K., & Ellegren, H. (1999). A simple and universal method for molecular sexing of non-ratite birds. *Journal of Avian Biology*, *30*(1), 116. <https://doi.org/10.2307/3677252>
- Goutte, A., Barbraud, C., Herzke, D., Bustamante, P., Angelier, F., Tartu, S., Clément-Chastel, C., Moe, B., Bech, C., Gabrielsen, G. W., Bustnes, J. O., & Chastel, O. (2015). Survival rate and breeding outputs in a high Arctic seabird exposed to legacy persistent organic pollutants and mercury. *Environmental Pollution*, *200*, 1–9. <https://doi.org/10.1016/j.envpol.2015.01.033>
- Grosbois, V., & Thompson, P. M. (2005). North Atlantic climate variation influences survival in adult fulmars. *Oikos*, *109*(2), 273–290. <https://doi.org/10.1111/j.0030-1299.2005.13774.x>
- Guilford, T., Freeman, R., Boyle, D., Dean, B., Kirk, H., Phillips, R., & Perrins, C. (2011). A dispersive migration in the Atlantic puffin and its implications for migratory navigation. *PLoS ONE*, *6*(7), e21336. <https://doi.org/10.1371/journal.pone.0021336>
- Hanssen, S. A., Gabrielsen, G. W., Bustnes, J. O., Bråthen, V. S., Skottene, E., Fenstad, A. A., Strøm, H., Bakken, V., Phillips, R. A., & Moe, B. (2016). Migration strategies of common eiders from Svalbard: implications for bilateral conservation management. *Polar Biology*, *39*(11), 2179–2188. <https://doi.org/10.1007/s00300-016-1908-z>
- Hill, R. D., & Braun, M. J. (2001). Geolocation by light level. In *Electronic tagging and tracking in marine fisheries* (Springer, pp. 315–330).
- Koenker, R. (2020). *Quantreg: Quantile Regression. R package version 5.75 (version 5.75)*. R package. <https://cran.r-project.org/package=quantreg>
- Léandri-Breton, D. J., Tarroux, A., Elliott, K. H., Legagneux, P., Angelier, F., Blévin, P., Bråthen, V. S., Fauchald, P., Goutte, A., Jouanneau, W., Tartu, S., Moe, B., & Chastel, O. (2021). Long-term tracking of an Arctic-breeding seabird indicates high fidelity to pelagic wintering areas. *Marine Ecology Progress Series*, *676*, 205–218. <https://doi.org/10.3354/meps13798>

- Lisovski, S., Bauer, S., Briedis, M., Davidson, S. C., Dhanjal-Adams, K. L., Hallworth, M. T., Karagicheva, J., Meier, C. M., Merkel, B., Ouwehand, J., Pedersen, L., Rakhimberdiev, E., Roberto-Charron, A., Seavy, N. E., Sumner, M. D., Taylor, C. M., Wotherspoon, S. J., & Bridge, E. S. (2020). Light-level geolocator analyses: A user's guide. *Journal of Animal Ecology*, *89*(1), 221–236. <https://doi.org/10.1111/1365-2656.13036>
- Lisovski, S., & Hahn, S. (2012). GeoLight - processing and analysing light-based geolocator data in R. *Methods in Ecology and Evolution*, *3*(6), 1055–1059. <https://doi.org/10.1111/j.2041-210X.2012.00248.x>
- Lisovski, S., Hewson, C. M., Klaassen, R. H. G., Kristensen, M. W., Hahn, S., Korner-Nievergelt, F., Kristensen, M. W., & Hahn, S. (2012). Geolocation by light: accuracy and precision affected by environmental factors. *Methods in Ecology and Evolution*, *3*(3), 603–612. <https://doi.org/10.1111/j.2041-210X.2012.00185.x>
- Miller, H. J. (1991). Modelling accessibility using space-time prism concepts within geographical information systems. *International Journal of Geographical Information Systems*, *5*(3), 287–301. <https://doi.org/10.1080/02693799108927856>
- Mysterud, A., Stenseth, N. C., Yoccoz, N. G., Langvatn, R., & Steinheim, G. (2001). Nonlinear effects of large-scale climatic variability on wild and domestic herbivores. *Nature*, *410*(6832), 1096–1099. <https://doi.org/10.1038/35074099>
- Neutens, T., Witlox, F., Van De Weghe, N., & De Maeyer, P. H. (2007). Space-time opportunities for multiple agents: A constraint-based approach. *International Journal of Geographical Information Science*, *21*(10), 1061–1076. <https://doi.org/10.1080/13658810601169873>
- Technitis, G., Othman, W., Safi, K., & Weibel, R. (2015). From A to B, randomly: a point-to-point random trajectory generator for animal movement. *International Journal of Geographical Information Science*, *29*(6), 912–934. <https://doi.org/10.1080/13658816.2014.999682>
- van Bemmelen, R. S. A., Kolbeinsson, Y., Ramos, R., Gilg, O., Alves, J. A., Smith, M., Schekkerman, H., Lehtikoinen, A., Petersen, I. K., Pórisson, B., Sokolov, A. A., Välimäki, K., van der Meer, T., David Okill, J., Bolton, M., Moe, B., Hanssen, S. A., Bollache, L., Petersen, A., ... Tulp, I. (2019). A migratory divide among red-necked phalaropes in the Western Palearctic reveals contrasting migration and wintering movement strategies. *Frontiers in Ecology and Evolution*, *7*, 86. <https://doi.org/10.3389/fevo.2019.00086>
- Woodworth, B. K., Wheelwright, N. T., Newman, A. E., Schaub, M., & Norris, D. R. (2017). Winter temperatures limit population growth rate of a migratory songbird. *Nature Communications*, *8*, 1–9. <https://doi.org/10.1038/ncomms14812>